This article has been accepted for publication in a future issue of this journal, but has not been fully edited. Content may change prior to final publication. Citation information: DOI 10.1109/TWC.2021.3057864, IEEE Transactions on Wireless Communications

I-Talk: Reliable and Practical Superimposed Signal Decoding without Power Control

Wen Cui, *Student Member, IEEE,* Chen Liu,
Wenjun Yang, *Student Member, IEEE,* and Lin Cai, *Fellow, IEEE*

***Abstract*—Internet-of-Things (IoT) is emerging, while the spectrum is at a premium. To enhance spectrum efficiency, a promising solution is Non-Orthogonal Multiple Access (NOMA) that enables users to communicate with the same resource at the same time, while decoding the superimposed signal at the receiver. Existing NOMA technologies, however, rely on strict power control to decode the superimposed signal, infeasible for heterogeneous and low-cost IoT devices. In contrast, we propose I-Talk, a new NOMA scheme that is designed for IoT and can decode the superimposed signals from two transmitters without power control. Importantly, considering the IoT systems in the wild, both the hardware imperfections and mobility are unavoidable, which can cause severe signal variations, resulting in an unreliable decoding performance. To solve this problem, we design a synthesis channel coefficient to track all signal offsets caused by the hardware imperfection. Meanwhile, we propose a diversity transmission and smart combining scheme to achieve high reliable decoding performance. To demonstrate the feasibility of this new NOMA approach in practical systems, we implement I-Talk with USRP devices and the experimental results illustrate that I-Talk achieves a one-order lower bit-error-rate and a 1.47× higher throughput gain than the state-of-the-art superimposed signal decoding scheme.**

***Index Terms*—Wireless Communication, Spectrum Efficiency, Superimposed Signals.**

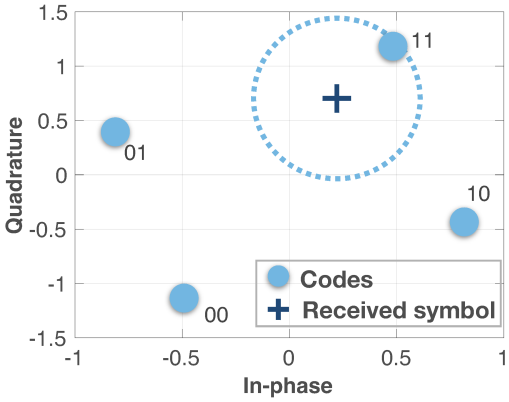

Fig. 1: Decoding the superimposed signal in modulation-level. In this example, we consider two concurrent transmitters using BPSK modulation for simplicity. When two BPSK modulated signal symbols from two transmitters arrive at the receiver, the receiver can decode the superimposed signal symbol by calculating the minimum Euclidean distance between the received signal symbol and the codes in the constellation map. In the above example, the decoding result is '11', which means that both of the transmitted signal symbols are '1'. Note that we use the terms demodulation and decoding interchangeably.

I. Introduction

A. Background

The unprecedented growth of the Internet-of-Things (IoT) comes with emerging communication demands [1], [2]. As a result, wireless spectrum is scarcer [3], [4]. To meet the increasing demand, it is critical to improve the spectrum efficiency. Traditionally, the spectrum is allocated orthogonal to each user in time/frequency/code domains [5]. But this allocation becomes less efficient for a massive number of IoT devices, and it can lead to severe spectrum competitions.

To increase spectrum efficiency, recent studies proposed Non-Orthogonal Multiple Access (NOMA) that enables multiple users to use the same spectrum at the same time and then the receiver decodes superimposed signals [6], [7]. Although promising, NOMA originated from cellular networks and is incompatible with many IoT applications. Specifically, to decode the superimposed signal, most NOMA technologies use the Successive Interference Cancellation (SIC) approach which requires a strict power control to maintain signal strength gaps among users. However, this precise power control may not be feasible for many IoT devices that are heterogeneous and often of low-cost.

Can we decode the superimposed signals for NOMA without the power control? To answer this question, we are inspired by the Physical-layer Network Coding (PNC) [8], [9], [10] that can decode superimposed signals in the modulation level without requiring any power control among users. The basic idea of this modulation-level decoding scheme is that each received signal symbol can be decoded by matching to the possible representative code in the constellation map as shown in Fig. 1. Since PNC requires to know one of the two concurrently transmitted signals, the number of the possible representative codes is halved, making it easier to decode. However, to decode superimposed signals from two users with NOMA, no signal is known in advance, so it is more more difficult to decode. Furthermore, considering the IoT

Manuscript received April 11, 2020; revised September 26, 2020 and December 14, 2020; accepted January 28, 2021. Date of publication XXX XX, 20XX; date of current version XXX XX, 20XX. This work was supported in part by NSERC, Compute Canada, and China Scholarship Council (CSC). (*Corresponding author: Lin Cai.)*

Wen Cui, Wenjun Yang, and Lin Cai are with the Department of Electrical and Computer Engineering, University of Victoria, Victoria, BC V8P 5C2, Canada. Email: wencui@uvic.ca, wenjunyang@uvic.ca, and cai@ece.uvic.ca.

Chen Liu is with the Department of Information Science and Technology, Northwest University, Xi'an, Shaanxi 710127, China, and also with the Department of Electrical and Computer Engineering, University of Victoria, Victoria, BC V8P 5C2, Canada. Email: liuchen@nwu.edu.cn

systems in the wild, both the hardware imperfections and the dynamic channel conditions can cause severe variations on the received signal symbols, resulting in an unreliable decoding performance. Therefore, a reliable modulation-level decoding scheme for IoT remains an open issue.

B. Challenges and Proposed Solutions

In this paper, we propose I-Talk, a new NOMA technology that can decode the superimposed signals from two concurrent transmitters in the modulation level without power control. I-Talk aims to achieve high reliability in the presence of hardware imperfections and mobile channel conditions. However, it is non-trivial to realize I-Talk due to the following practical challenges.

- First, to decode the superimposed signal in the modulation level, symbol-level synchronization is required in both the time and frequency domains, i.e., signals from the two users should arrive at the receiver simultaneously and on the same frequency. However, synchronizing IoT devices in the presence of hardware imperfections and mobile channel conditions is non-trivial. This is mainly because the hardware imperfections can cause unpredictable signal offsets in the time, frequency, and phase domains. Moreover, the mobility together with the Doppler effect from the mobile IoT devices can cause extra signal offsets compared to static scenarios, which deteriorates the synchronization accuracy.
- Second, decoding the superimposed signal from the modulation level is intrinsically difficult in matching the location of the received signal symbol to its representative code precisely. In particular, both the hardware imperfections and mobility can cause severe signal variations, so that some codes in the constellation map are too close to each other and cannot be distinguished clearly, resulting in an unreliable decoding performance.

To deal with the above challenges, we first study the signal offsets caused by the hardware imperfection and mobility, i.e., the Carrier Frequency Offset (CFO), the Sampling Frequency Offset (SFO) and the Sampling Time Offset (STO), and design a synthesis channel coefficient to represent all these offsets. By doing so, we can trace all the offsets and then eliminate the side effects of these offsets, providing a stable synchronization performance. Second, by exploiting the complementary property of the representative codes and the subcarriers' differences in complicated channel environments as well as the substantial diversity gain of transmitting two copies of the signal, we propose a diversity transmission and smart combining scheme to achieve high reliable decoding performance.

The main contributions of this paper are as follows:

- We derive a synthesis channel and based on this design, I-Talk can achieve near-perfect synchronization for IoT devices in the presence of the hardware imperfections and mobile channel conditions.
- We propose a reliable superimposed signal decoding approach for NOMA without any power control. Moreover, with the proposed diversity transmission and smart combining scheme, I-Talk can achieve high reliability regardless of the hardware imperfections and mobility in both static and mobile IoT systems.
- We implement I-Talk on a software-defined radio platform and evaluate its performance across various scenarios. Our extensive experimental results demonstrate that I-Talk achieves a one-order lower bit-error-rate and a 1.47× higher throughput gain in the mobile scenario, outperforming the state-of-the-art scheme.

C. Related Work

Non-Orthogonal Multiple Access (NOMA). NOMA technology aims to better utilize the spectrum by enabling multiple users to transmit their signals using the same wireless spectrum, i.e., at the same time and on the same frequency [6], [7], [11]. To implement NOMA in practice, it requires a considerable large signal power gap between different users, so that each signal can be separated in the power domain [12], [13]. Although promising, when it comes to heterogeneous and often low-cost IoT devices, the signal power gap cannot be maintained due to the complexity and hardware imperfection, making the existing NOMA technologies infeasible to many IoT systems, which motivated this work.

Physical-layer Network Coding (PNC) and Analog Network Coding (ANC). PNC [8], [9], [10], [14], [15], [16] and its counterpart solution ANC [17] have drawn many attentions recently in the superimposed signal decoding for relay networks. These solutions can be adopted for relay system where the receiver knows one of the two signals superimposed, and then the unknown signal can be decoded by removing the known signal from the superimposed signal. PNC decodes the superimposed signal in modulation-level from the constellation map, while ANC decodes in analog-level by canceling out the known signal. Both cannot be extended to multiple access scenarios. Furthermore, existing PNC and ANC are dedicated to static scenarios, and may encounter a performance degradation in the presence of mobility.

Decoding superimposed signals for low data rate technologies. Many recent work focus on decoding superimposed signals in low data-rate technologies, such as RFID [18], LoRa [19], ZigBee [20] by leveraging their spread-spectrum feature or over-sampling long symbols. But these solutions cannot be utilized by other general data-rate systems, such as Wi-Fi. I-Talk focuses on OFDM, which is feasible for many technologies with a general date rate, e.g., IEEE 802.11.

Space-time codes. The space-time code is applied in the literature to obtain a diversity gain, such as the Alamouti Code [21], [22], [23]. But it requires multi-antenna to transmit the coded symbol, which may not always be feasible or desirable for IoT devices. We notice that some work studied the use of space-time code for concurrent users in theory [24]. However, the work requires perfect knowledge of the Channel State Information (CSI) before each transmission and neglects the influence of the hardware noises. As a result, a varying channel in practice may lead to its performance degradation. In I-Talk, we aim to design a practical NOMA scheme for IoT, and therefore we make no assumption on the CSI and work well for a single-antenna system. On the other hand, when

This article has been accepted for publication in a future issue of this journal, but has not been fully edited. Content may change prior to final publication. Citation information: DOI 10.1109/TWC.2021.3057864, IEEE Transactions on Wireless Communications

the IoT devices do have multiple antennas, it is possible to combine both space-time codes and I-Talk technologies for a better performance, as they are orthogonal.

II. I-Talk Overview

I-Talk is designed to decode the superimposed signal for IoT systems, aiming to achieve high reliability in the presence of mobility and hardware imperfections. I-Talk first addresses several critical issues in practice, including the time, frequency and phase synchronizations in the mobile scenario with hardware imperfections. Next, I-Talk investigates the underlying reasons of the decoding error for superimposed signals, and reveals a complementary property of the decoding error in the constellation map. Based on that, I-Talk designs a diversity transmission and smart combining decoding scheme for superimposed signals to guarantee high reliability. We elaborate on the above components and provide the technical details in the next few sections.

Note that our current system is aiming to improve the communication performance from the design of the physical layer, such as the encoding and decoding process. We are aware that the current work is lacking the description of MAC-layer details which are beyond the scope of this work. But we understand that the MAC protocol is a critical further research issue. Therefore, we provide some initial thoughts as follows.

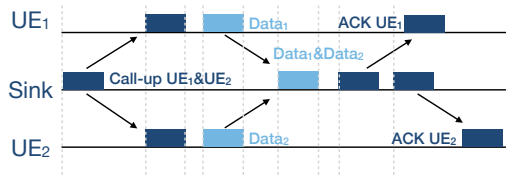

Fig. 2: An illustrative example of the transmission process.

For distributed transmissions, we have seen a growing interest in improving the diversity gain from multiple concurrent transmitters in a distributed manner [25], [26], [27]. In particular, at the first stage of the transmission, a lead transmitter will call up a transmission, and one slave node with the first reply will be selected to join in the transmission as another party of the two-user concurrent transmission. Note that the selection of the slave node has also been well-studied in the area of opportunistic routing for ad-hoc wireless networks [28]. For central control transmissions, although the end users of many IoT applications are low-cost, e.g. wireless sensor networks [29], the sink node or gateway node is capable of scheduling the transmission of low-cost devices. For example, the concurrent transmission from two low-cost sensor nodes can be scheduled by the sink node, by which the collision can be avoided and the latency can be reduced. An illustrative example is shown in Fig. 2.

III. Practical Challenges in Decoding Superimposed Signals

I-Talk is proposed to decode the superimposed signal in modulation-level. To achieve that, the system requires an accurate estimation of the signal variation before decoding. However, in practice, the hardware imperfection and mobility will decrease the estimation accuracy significantly. In particular for a superimposed signals, the decrease of the estimation accuracy would result in a much higher decoding error. To address that, we first illustrate the preliminary of the superimposed signal. Second, we study the key factors in affecting the estimation accuracy. Last, we propose a solution to improve the the estimation accuracy in the presence of the mentioned practical challenges.

A. Preliminary

Considering the basic case of two concurrent transmitters, the received superimposed signal Y can be represented as

$$Y = H_1 X_1 + H_2 X_2 + N, \tag{1}$$

in the frequency domain. Here, X_1 and X_2 are the transmitted signals, and H_1 and H_2 are the corresponding channels between the two transmitters and receiver, respectively. N refers to the white Gaussian noise. Eq. 1 is valid in an ideal scenario where the channel is the only factor to cause signal variations, without considering the hardware imperfection. In practice, precisely measuring the channel is the key to successful decoding. Indeed, decoding the superimposed signal demands a high synchronization accuracy in the time, frequency and phase domains [8].

First, symbol-level time synchronization is needed [8], [9], [10] for decoding the superimposed signal. Specifically, by using IEEE 802.11p as an example, the time synchronization error should be no larger than 2 μs. Recent work has shown that this level of synchronization is achievable on off-the-shelf devices, e.g., a 300 ns accuracy for outdoor scenarios can be achieved by GPS clocks [30]. For simplicity, we use a commercial GPS clock to achieve the required time synchronization. More details are presented in Sec. VI. Second, besides the time synchronization, due to the highly mobile channel conditions and hardware imperfections, various signal offsets deteriorate the frequency and phase synchronizations, making decoding superimposed signals non-trivial. In the following, we focus on these unsolved synchronization problems, and assume the time synchronization have been well achieved.

B. Vital Factors of the Signal Variation Estimation

For a single pair of transmitter and receiver, decoding a signal require us to deal with three offsets at the receiver [31], [32]: the Carrier Frequency Offset (CFO), the Sampling Frequency Offset (SFO) and the Sampling Time Offset (STO). Generally, CFO and SFO exist because of the differences between the internal oscillators, and STO is caused by signal detection failures [33]. To correct these offsets, a precise offsets measurement is needed at the receiver. But the mobile channel condition and hardware imperfections make the precise offsets measurement hardly achievable, even using the GPS clock [30], [34]. Moreover, concurrent transmitters cause more offsets and make channel conditions more complicated.

Signal offsets. To see these offsets clearly, we conduct a benchmark experiment with two USRP devices as a transmitter and a receiver deployed in two vehicles, respectively. Each

This article has been accepted for publication in a future issue of this journal, but has not been fully edited. Content may change prior to final publication. Citation information: DOI 10.1109/TWC.2021.3057864, IEEE Transactions on Wireless Communications

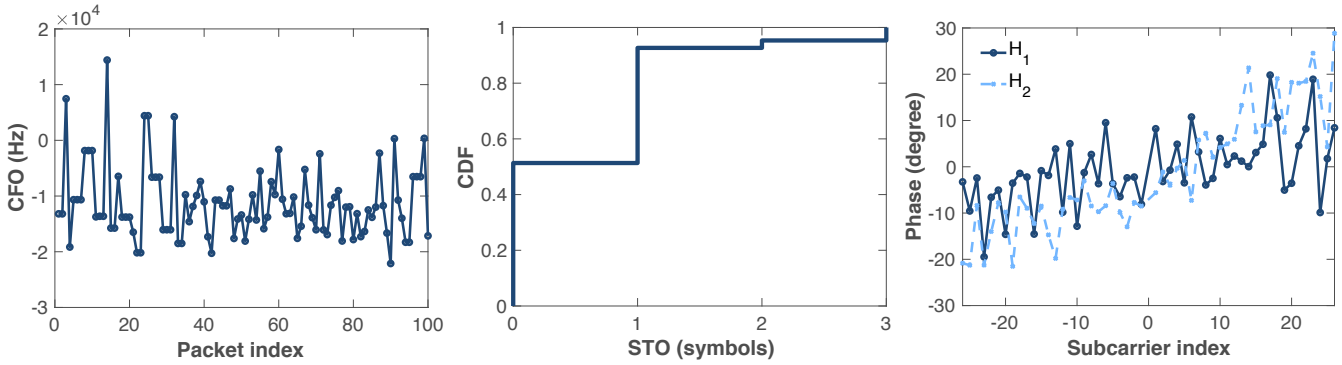

(a) CFO. (b) STO. (c) SFO.

Fig. 3: Signal offsets in the mobile scenario with Doppler effect.

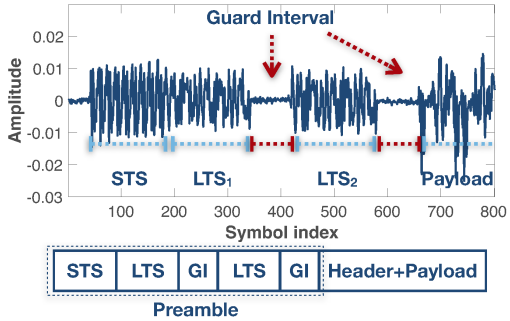

Fig. 4: Preamble and packet formats.

device connected to a GPS clock for synchronization. The signal is operating at 5.9 GHz carrier frequency with 10 MHz bandwidth, and the synchronization error under ideal condition is around ± 50 ns. The more detailed setup is introduced in Sec. VI-A. Specifically, Fig. 3a shows that CFO has a large fluctuation up to 3.5 KHz in the presence of the Doppler effect and the hardware imperfection. Fig. 3b plots the mismatch in terms of symbols for STO. This mismatch would not directly cause a synchronization failure, but it would lead to more phase offsets, making the signal hard to be decoded successfully. Note that the symbol and the sample are used interchangeably as no oversampling is assumed in our system. The probability of a successful match is only 50% due to mobility. Fig. 3c shows that there is a large phase variation for SFO caused by mobility and hardware imperfections. Note that CFO affects the frequency synchronization, while SFO and STO damage the phase synchronization. Therefore, to decode the superimposed signal, we need to track and react to these offsets using precise channel measurements.

Preamble design. To ensure precise packet detection and channel measurement, each packet should start with a preamble, which is also critical for handling the three offsets. In IEEE 802.11p, a preamble containing a Short Training Sequence (STS) for the packet detection and a Long Training Sequence (LTS) for measuring the channel condition and the three offsets. However, LTS can be easily be collided under concurrent transmissions. To understand this more clearly, we start from introducing the procedure of the use of LTS. Specifically, once a signal is detected by a receiver via STS, the receiver will apply an FFT operation with an FFT window to capture LTS. Because LTS is predefined in advance, the comparison between the received LTS and the transmitted LTS would reveal the signal variations that caused by the channel condition and the offset. In a single transmitter system, it is straight-forward to capture LTS with the FFT window. But for a system with two concurrent transmitters, especially with mobility, different LTS may collide with each other due to the propagation delay and hardware processing delay, and then the FFT window would later capture a mixed LTS from two transmitters. As a result, the receiver cannot distinguish the signal variations caused by the interruption of other LTS from the variations caused by the channel condition and the offsets, making the following procedure unable to react accurately. To address this problem, we insert two extra NULL symbols as the guard intervals shown in Fig. 4 to enlarge the distance of two transmitted signals in the time domain. By doing so, although LTS from different transmitters may have time-domain shifts caused by the mentioned delays, the guard intervals provide a robust range to avoid the collision of LTS in practice. The newly added NULL symbols are sufficient for addressing the LTS collision problem and the additional overhead is negligible as detailed in Sec. V. Note that during a packet transmission time, e.g., 1 ms, the channel distance and propagation delay changes of due to user mobility (in nano-second level) are negligible, which will not affect I-Talk performance. In the following design of I-Talk, we will use the proposed preamble as our default settings.

In our design, the performing of the decoding relies on an aligned preamble between two users and the allocated pilot subcarriers should be known in advance. Note that given the existing feedback used in infrastructure-based IoT systems, such as 3GPP, the additional bits to notify the settings of I-Talk in the feedback message are negligible.

C. Synthesis Channel Estimation

Next, we describe the mathematical representation of the superimposed signal at a receiver. For a received sample $r(t_n)$, it contains a summation of two signals, s_1 and s_2, and the white Gaussian noise n_0. Due to the offsets, more changes will be reflected on the received signal beyond the channel response. Specifically, Δf_i causes CFO, and $n_{i\epsilon}$ causes STO,

This article has been accepted for publication in a future issue of this journal, but has not been fully edited. Content may change prior to final publication. Citation information: DOI 10.1109/TWC.2021.3057864, IEEE Transactions on Wireless Communications

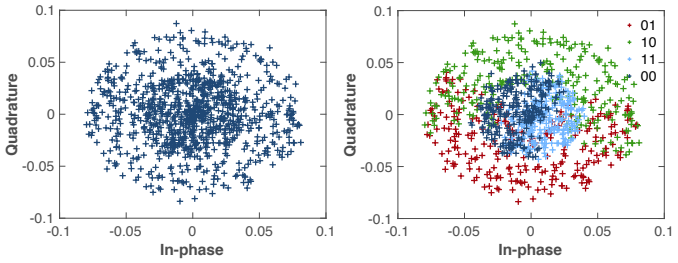

(a) Without synthesis channel. (b) With synthesis channel.

Fig. 5: The constellation map of the received signal.

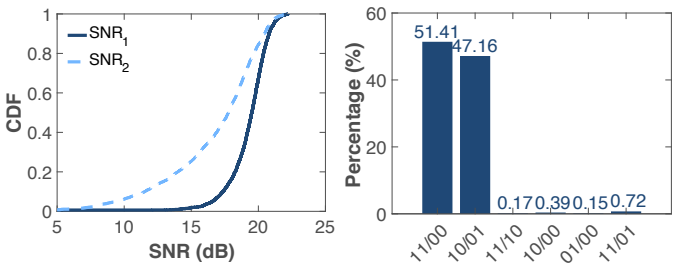

(a) SNR. (b) Error distributions.

Fig. 6: Benchmark experiment results. "11/00" represents that "11" is mistakenly decoded as "00" and vice versa.

and then the received superimposed signal can be represented as

$$r(t_n) = e^{j2\pi\Delta f_1 n T_1} \sum_i h_{1i}(nT_1')(s_1(n-n_{1\epsilon})T_1' - \tau_{1i}) + e^{j2\pi\Delta f_2 n T_2} \sum_i h_{2i}(nT_2')(s_2(n-n_{2\epsilon})T_2' - \tau_{2i}) + n_0, \quad (2)$$

where T_i' and T_i are the sampling time at the receiver and the transmitter (i.e., SFO), respectively [33], and h_i and τ_i are the channel impulse response and the delay, respectively.

Although CFO, STO and SFO are caused by different reasons, all of them induce a phase shift to the signal. These phase shifts can be described as

$$\theta_n^{k,CFO} = 2\pi\Delta f n T, \quad (3)$$

$$\theta_n^{k,STO} = 2\pi k n_\epsilon / N_d, \quad (4)$$

$$\theta_n^{k,SFO} = 2\pi k\gamma(N_d + L)/N_d, \quad (5)$$

where n refers to the n-th sample of the signal sequence and k is the k-th subcarrier index of one OFDM symbol. $\gamma = (T - T')/T$ is defined as the sampling time error ratio, and L the length of the Cyclic Prefix (CP), and N_d the length of the data part in every OFDM symbol. Here, we can use CFO error ratio $\epsilon = \Delta f/f$ to infer SFO error ratio γ. We assign two pilot samples for each transmitter to keep tracking the varying offsets in every symbol. Overall, the total phase shift can be written as

$$\theta_n^k = \theta_n^{k,CFO} + \theta_n^{k,STO} + \theta_n^{k,SFO}. \quad (6)$$

One thing worth noting is that for a single transmitter, the offsets can be measured first and compensated later. However, for a superimposed signal, compensating the offset for one transmitter would hurt the other, since the offsets from different transmitters have different characters. To solve this problem, instead of compensating the signal, I-Talk combines the channel conditions and the offsets to define a synthesis channel $\mathcal{H}$,

$$\mathcal{H} = He^{j\theta_n^k}, \quad (7)$$

which can enable the receiver to decode the signal dynamically according to the channel condition and the offsets.

By using the BPSK modulation as an example, we have four combinations representing "11", "00", "10" and "01". As shown in Fig. 5a, in the presence of offsets and varying channel conditions, the signal from the concurrent transmitters do not have a constant phase relationship with each other, resulting to a varying constellation map over time. In contrast, with the proposed synthesis channel, we can precisely track the varying pattern of the constellation map to identify the combinations of the superimposed signal which is shown in Fig. 5b labeled by different colors.

IV. Understanding the Decoding Error

A. Decoding Error Analysis

To deal with the decoding error, existing solutions employ packet retransmissions [35], [36], [12], [11], [37]. However, the retransmission may introduce extra communication overhead and long delay, which is not desirable for many IoT applications. To design a reliable decoding scheme and reduce the decoding error, we start by understanding what are the specific decoding errors and where are these errors from.

Signal variations in the IQ domain. We conducted a benchmark experiment with the same setting in Sec. III-B. OFDM with the BPSK modulation is used for communications. The varying channel during the experiment is represented by the SNRs of the two transmitters shown in Fig. 6a. When two BPSK modulated signals arrive at a receiver concurrently, four possible combinations exist in the IQ domain, representing "11", "10", "01" and "00". A decoding error happens when the received signal is misidentified as wrong combinations by the receiver. Fig. 6b shows the decoding error distribution, which is calculated from more than 2500 concurrently transmitted packets. Obviously, in most cases, it cannot distinguish "11" from '00" and "10" from "01" with the percentage of 51.47% and 47.16%, respectively. Furthermore, we observe that the positions of the codes may change and become too close to be distinguished (Fig. 7c and Fig. 7d) due to the signal variation caused by dynamic channel conditions and hardware imperfections, which will be exacerbated in mobile scenarios. *This observation implies that controlling the positions of the codes is the key to reduce the decoding error.* Specifically, we focus on reducing the decoding errors of "11/00" and "10/01" since these two error cases account for a dominant portion (i.e, 98.63%) of all error cases.

Impact factors of the codes position. The positions of the codes in the constellation map and the decoding error probability are mainly determined by two factors: the amplitude of both signals ($|H_1|$ and $|H_2|$) and the phase difference ϕ of the two signals. More detailed quantitative analysis and BER

This article has been accepted for publication in a future issue of this journal, but has not been fully edited. Content may change prior to final publication. Citation information: DOI 10.1109/TWC.2021.3057864, IEEE Transactions on Wireless Communications

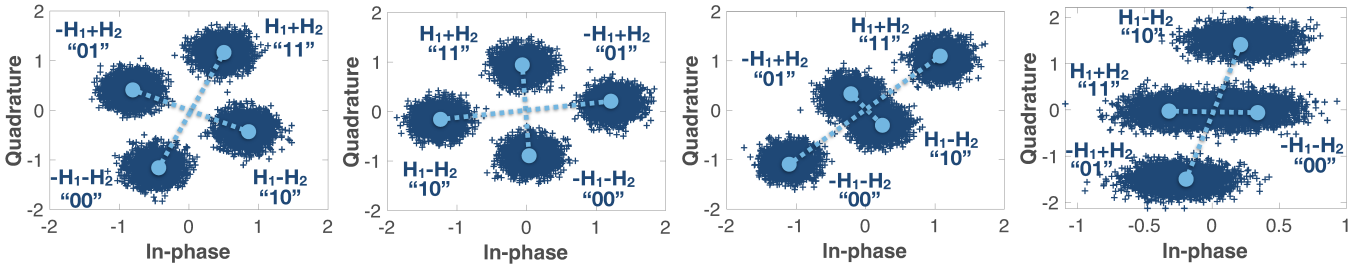

(a) Distinguishable case 1. (b) Distinguishable case 2. (c) Indistinguishable case 1. (d) Indistinguishable case 2.

Fig. 7: Position variation of received symbols in the constellation map.

expression can be found in [38], [39]. To further understand the effect of each factor on the decoding performance, we plot the BER heatmaps under different SNRs and phase differences in Fig. 8 via Monte Carlo simulations. Here, we use SNR instead of $|H|$ since SNR is a common metric for signal amplitude. We observe the following property:

Given SNR_1 and the SNR ratio, the lower BER and higher BER appear alternatively as the phase difference ϕ varies from 0° to 360°. The best choice of ϕ for the lower BER is centered around 90° or 270° (defined as 'good regions'). In contrast, the higher BER occurs when ϕ is centered around 0° or 180° (defined as 'bad regions'). Furthermore, the three BER heatmaps have the same trend as SNR_1 varies from 6 dB to 12 dB, which indicates that the positions of 'good regions' and 'bad regions' are not affected by SNR values. Note that by using this knowledge of 'good regions' and 'bad regions', a receiver can directly anticipate the possible BER range through measuring the phase difference ϕ with the preamble.

B. Manipulating the Phase Difference

The above property motives us to manipulate the phase difference ϕ for a good decoding performance [1].

Complementarity between "11/00" and "10/01". Recall that our goal is to reduce the decoding errors of "11/00" and "10/01" cases. So, we zoom in on the two 'bad regions' (i.e., $\phi = 0^\circ, 180^\circ$) for "11/00" and "10/01" cases, respectively.

Apparently, as shown in Fig. 7d, when "11" and "00" cannot be distinguished easily, the distance between code "11" and code "00" (denoted as $d_{11/00}$) is small. The similar situation for "10/01" case can be observed in Fig. 7c. Thus, we need to manipulate the phase difference of the transmitted signals to adjust $d_{11/00}$ and $d_{10/01}$ in the constellation map.

To change the phase difference, for simplicity, we assume H_1 is fixed and then rotate H_2 from point a to b, c, d as shown in Fig. 9a. Apparently, $d_{11/00}$ gets its maximum value $2(|H_1|+|H_2|)$ and minimum value $2(|H_1|-|H_2|)$ when H_1 and H_2 are in the same direction (point a) and the opposite direction (point c), respectively. In contrast, $d_{10/01}$ gets its maximum value and minimum value at point c and a, respectively. Furthermore, Fig. 9b shows the variation trend of $d_{11/00}$ and $d_{10/01}$ with respect to different phase differences. We obtain the following complementary property:

The two 'bad regions' for "11/00" and "10/01" are complementary to each other. Specifically, when it is difficult to distinguish "11" from "00", "10" and "01" can be distinguished easily, and vice versa. To further validate the complementary property, we conduct simulations based on the BER expression [38] and plot the BER curves in Fig. 9c. We observe that the 'bad region' with $\phi = 0^\circ$ (denoted as $\text{bad}_{10/01}$) is only bad for the "10/01" case, while it is actually good for the "11/00" case. Similarly, the 'bad region' with $\phi = 180^\circ$ (denoted as $\text{bad}_{11/00}$) is bad for "11/00", but good for "10/01".

V. A Reliable Decoding Scheme

In this section, we propose a reliable approach for decoding the superimposed signal in the presence of the hardware imperfection and mobility.

A. Rotation Code Based Diversity Transmission

The observation mentioned above motivates us to leverage the complementary property to reduce the decoding error. Specifically, our idea is to explore the diversity gain to let each node transmit two copies of the signal within one transmission. If we can control the phase difference of the first copy pair (ϕ_A) to fall into $\text{bad}_{11/00}$ and the phase difference of the second copy pair (ϕ_B) in $\text{bad}_{10/01}$, we can perfectly eliminate these two error cases when combining the two copies for decoding. Here, we assume the two concurrent transmitters transmit two copies of their signals sequentially. At the receiver, it would receive the two superimposed signal copies from the two transmitters. Hence, we denote the phase difference of the first copy as ϕ_A, and the second as ϕ_B.

However, in practice, it is challenging to precisely manipulate the phase difference into the specific 'bad regions' due to the large initial phase noise in many devices [40], [41]. Indeed, we cannot precisely control the values of ϕ_A and ϕ_B. Our solution is that, first, we need to guarantee $\phi_A \neq \phi_B$. To do so, we rotate the second copy of one transmitted signal with a certain angle α, while keeping the other copies unchanged, i.e., $\phi_B = \phi_A + \alpha$. Here, we can safely assume that the angle relationship is consistent within one packet [5]. Second, if one phase difference (ϕ_A or ϕ_B) is in one 'bad region', we need to let the other phase difference in the complementary region. To this end, we observe that the distance between two 'bad

[1]In fact, we can either control the SNR or the phase difference to achieve a lower BER. However, controlling signal amplitude requires strict power control which may be impractical for most IoT devices that are heterogeneous and often low-cost.

This article has been accepted for publication in a future issue of this journal, but has not been fully edited. Content may change prior to final publication. Citation information: DOI 10.1109/TWC.2021.3057864, IEEE Transactions on Wireless Communications

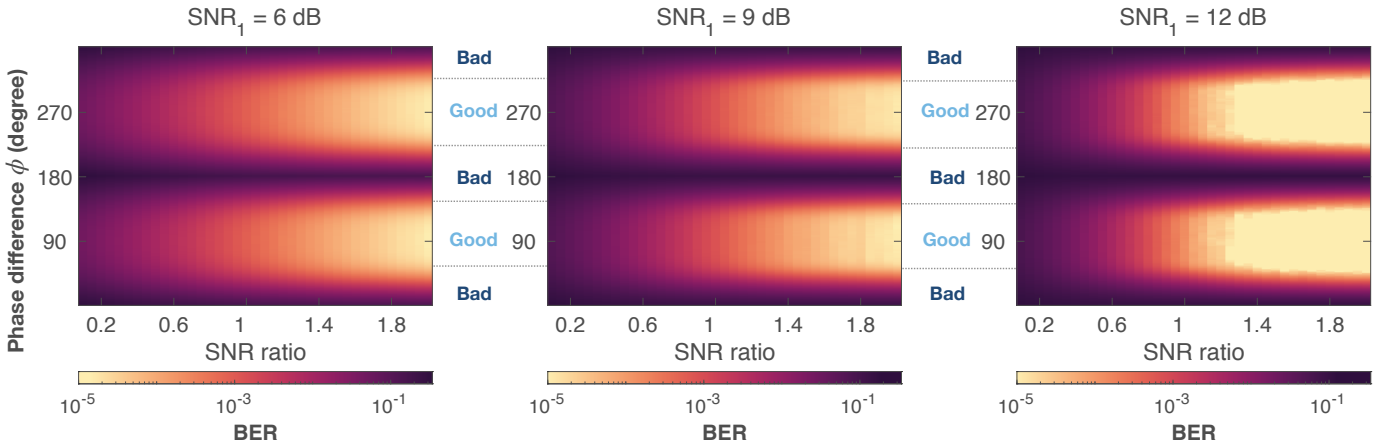

Fig. 8: Decoding performance under different SNRs and phase differences. SNR ratio is defined as $\mathrm{SNR}_2/\mathrm{SNR}_1$.

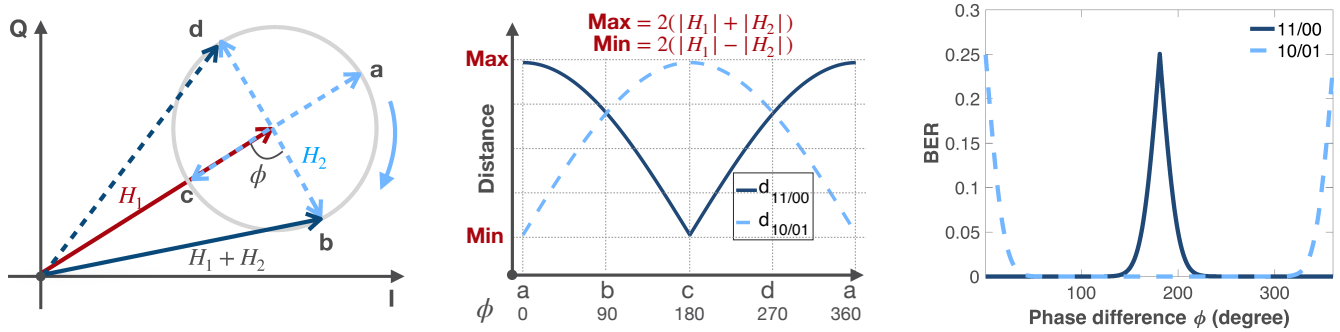

(a) (b) (c)

Fig. 9: Conceptual illustration of the complementarity between "11/00" and "10/01": (a) H_2 rotates from point a to b,c,d, and distances $d_{11/00}$ and $d_{10/01}$ vary accordingly. (b) $d_{11/00}$ and $d_{10/01}$ fragments with respect to different positions (i.e., different phase differences ϕ). (c) Theoretical results from the BER expression.

regions' is $180°$ and the BER curve is monotonous from one 'bad region' to its adjacent 'good region' (Fig. 9c). Therefore, we find the optimal rotating angle α to be $180°$.

B. Smart Combining

At the receiver side, for each copy, the received symbols can be decoded following the minimum Euclidean distance scheme in the IQ domain as described in Section I shown in Fig. 1. So, we have two decoding results for each received symbol, say $\hat{X}_A$ and $\hat{X}_B$. *Which one should be selected as the final decoding result or how to combine these two results?*

Decoding selection. Intuitively, we can employ Maximum Ratio Combining (MRC) to combine these two results. However, MRC performs well when the constellation map is regular and the same for all copies [42], [43]. Due to the mobile channel conditions and hardware imperfections, the constellation maps become irregular and different. So, we cannot directly use the MRC approach. Another possible solution is to assign weights to each result based on the Error Vector Magnitude (EVM). However, this solution normally requires a stable channel condition and a high SNR [44], [45], which may not be available in mobile scenarios.

Our idea is to leverage the complementarity between "11/00" and "10/01". Specifically, if $\hat{X}_A$ equals $\hat{X}_B$, we can directly obtain the final result $\hat{X} = \hat{X}_A = \hat{X}_B$. Otherwise, if ϕ_A is in a 'good region', we can trust the first copy and use $\hat{X}_A$ as the final decoding result. But, if ϕ_A is in a 'bad region', we need to check this 'bad region' specifying $\mathrm{bad}_{11/00}$ or $\mathrm{bad}_{10/01}$. If $\hat{X}_A$ is not in the code set that this 'bad region' specified, we can still trust $\hat{X}_A$. Otherwise, we will trust $\hat{X}_B$.

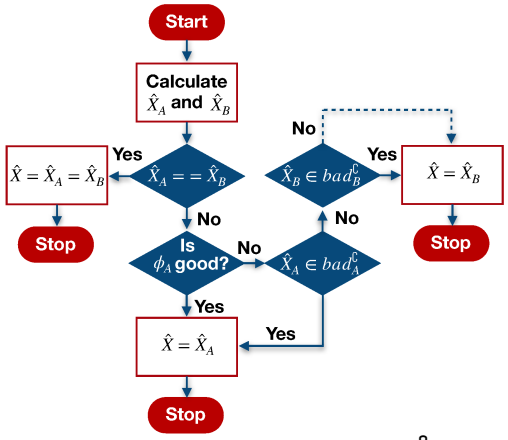

Fig. 10: Process of decoding selection. $\mathrm{bad}_A^{\mathbf{C}}$ refers to the complementary set of the codes that this 'bad region' specified. For example, if ϕ_A is in $\mathrm{bad}_{11/00}$, $\mathrm{bad}_A^{\mathbf{C}}$ contains "10" and "01".

The procedure is illustrated in Fig. 10.

Subcarriers' diversity. For 802.11p, using OFDM, the channel behaviors of different subcarriers are different due to the hardware imperfections and the frequency selective fading [46], [47]. Furthermore, the mobile channel conditions exacerbate the differences among subcarriers. To see this clearly, we conduct a benchmark experiment. Fig. 11 plots ϕ of one signal copy pair within one packet for different subcarriers. Clearly, the values of ϕ vary among subcarriers. In some subcarriers, ϕ is around 90° or 270°, which is in a 'good region'; in other subcarriers, ϕ is around 0° or 180°, which is in the 'bad region' for "10/01" or "11/00", respectively. Fig. 12 plots ϕ for different subcarriers under different time index (represented by the packet index). Apparently, even for the same subcarrier, ϕ is not stable and varies with time.

Algorithm 1: Smart Combining.

Result: The set of final decoding results, $\hat{X} = \{\hat{X}^k_{[i]}\}$.
for $i = 1$ **to** number_of_symbols **do**
  for $k = 1$ **to** number_of_subcarriers **do**
    if *(*$\hat{X}^k_{A[i]} == \hat{X}^k_{B[i]}$*) or (*$\phi^k_{A[i]} \in R_{good}$*) or (*$\hat{X}^k_{A[i]} \in bad^{\complement}_{A[i]^k}$*)* **then**
      $\hat{X}^k_{[i]} = \hat{X}^k_{A[i]}$;
    else
      $\hat{X}^k_{[i]} = \hat{X}^k_{B[i]}$;
    end
  end
end

The above experimental results reveal that the phase difference not only varies with subcarriers but also with time. Therefore, we need to apply the above decoding selection approach for every subcarrier at any given time. For simplicity, we summarize the smart combining in Algorithm 1. I-Talk system can keep the packet-level structure intact so our design can be readily adopted together with the existing error control mechanisms, such as using ACK and retransmission. After I-Talk decodes the superimposed signal from two users, the receiver will check the CRC of both the received packets. Next, at the ACK time slot, the receiver will broadcast the packet sequences that it has successfully received, and then the transmitter will decide whether to transmit new packets or retransmit the previous one. This decision is independent of the other transmitter, which makes I-Talk easy to implement.

C. Analysis

The orthogonal preamble. In the preamble design, the two LTS from each concurrent transmitter are orthogonal to each other in the time domain, which only introduces a small extra overhead. For example, for an 802.11p packet with 1460 bytes, and 6 Mbps transmission rate, the extra overhead is only 2.1% for two concurrent transmitters.

The overhead of the smart combining. I-Talk requires a traversal procedure of the packets to complete the smart combining. As the procedure can be piggybacked to the signal decoding component, the overhead is linearly increased and limited by the packet length. For the transmission part, at first glance, our scheme seems to introduce an extra overhead as we transit two repetitive symbols within in one packet, and therefore although we enable two users to transmit their packet at the same time, the overall throughput may equal to the back-to-back transmission of two users. In practice, our scheme can outperform back-to-back transmission, and we explain this in three-folds.

First, current IoT wireless communications often experience complicated fading channels, so to conquer this challenge, many IoT standards and protocols [48], [49], [50], [51] require users to blindly transmit their packets multiple times so that at least one of the packets can be correctly received. For example, the 3GPP standard requires the blind retransmission of multiple times for IoT/machine-to-machine transmissions given different SNR [49]. Under this design principle, we actually need to compare our scheme with the back-to-back transmission that includes a blind retransmission, and I-Talk can achieve a much higher throughput.

Second, our solution zooms in to the particular characters of the superimposed signal, and we develop encoding and coding schemes accordingly which offers a superior communication performance. Therefore, when compared with other concurrent transmission schemes that rely on retransmission [10], [12], our scheme aims to successfully decode the superimposed signal in the first place, which saves the transmission energy and spectrum.

Third, our current implementation uses repeating symbols to obtain a diversity gain. By doing this, the decoding accuracy can be enhanced. To further improve the performance of our design, more sophisticated coding strategies can be combined with our encoding part. Here we use the rotational coding [5] as an example. In a nutshell, the rotational code would encode two symbols from two consecutive packets with a rotation matrix, and by doing this, the receiver can decode both of the two transmitted symbols as long as one of the symbols is correctly decoded, which offers a diversity gain plus a coding gain. Therefore, we can use this newly obtained coding gain to compensate our cost of the diversity gain, and eventually offers even higher throughput gain when competing with back-to-back transmission without blind transmission. We see this as a promising direction, and we will investigate it in our future work.

Capacity regions. In this paper, we introduce I-Talk a NOMA technology, for enabling two users to transmit their packets at the same spectrum resources simultaneously. Our current implementation of I-Talk is compared with IoT communication that enables blind transmission, and the results in Fig. 13 show that I-Talk, by using half of the channel resources, the BER is below 10^{-4} when SNR is higher than 10 dB. In particular, in Fig. 13, we compare the average BER of two concurrent users between the NOMA scheme with SIC and with I-Talk, and we also plot the theoretical and simulation results of the BPSK modulation for a singular transmitter as a reference. Note that the results are based on a case that both of the received signal SNR are identical, and under such a case, the SIC would perform much worse compared with

This article has been accepted for publication in a future issue of this journal, but has not been fully edited. Content may change prior to final publication. Citation information: DOI 10.1109/TWC.2021.3057864, IEEE Transactions on Wireless Communications

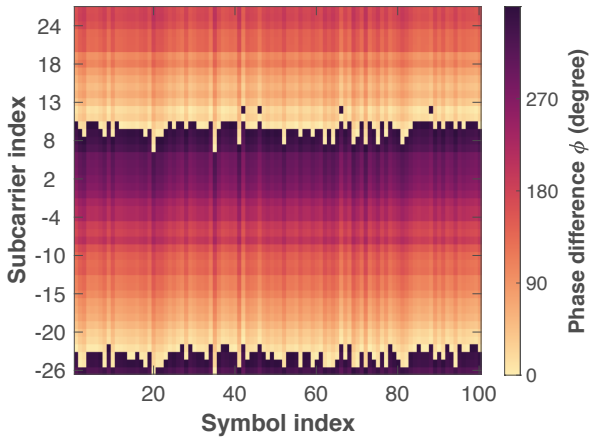

Fig. 11: Subcarriers' diversity within a packet.

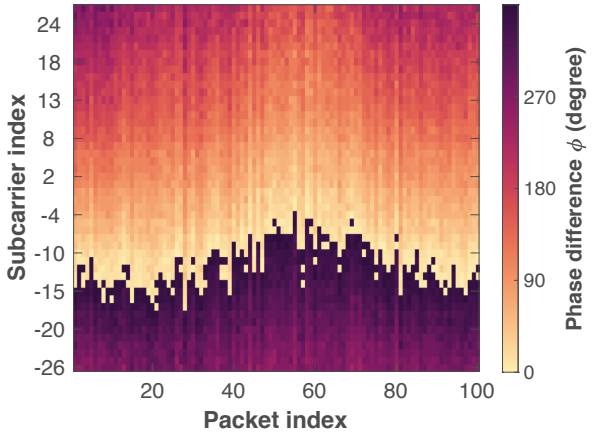

Fig. 12: Subcarriers' diversity among packets.

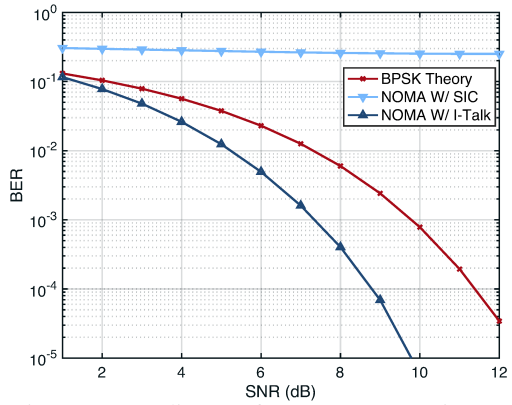

Fig. 13: Decoding performance comparisons.

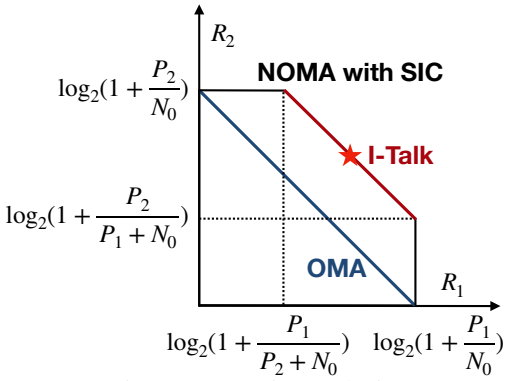

Fig. 14: Capacity analysis.

the performance of I-Talk, and we will detail the reason as follows.

The capacity analysis of OMA and NOMA with SIC have been well-studied in the literature [5]. Here, we start from some of the concepts of these knowledge and then explain our scheme. For traditional two-user OMA schemes, such as FDMA, TDMA, and CDMA, the capacity is limited by the user's capacity region. For example, under AWGN channels, the capacity regions for user 1 at a communication rate R_1, user 2 at a communication rate R_2 can be found as

$$\begin{cases} R_1 \leq W \log_2(1+\frac{P_1}{N_0}), \\ R_2 \leq W \log_2(1+\frac{P_2}{N_0}), \end{cases} \tag{8}$$

where W is channel bandwidth in Hz, P_1 and P_2 are the received power for user 1 and user 2, respectively, and N_0 denotes the power spectral density of the white Gaussian noise. Since OMA schemes need to divide the channel resource, an increased share and rate for user 1 will lead to a decreased for user 2, and the overall performance can be seen in Fig. 14.

Instead of competing for the spectrum resources, NOMA aims to let the two users access the channel simultaneously with some mutual interference. As a result, a new capacity region for the sum of two users can be represented as

$$R_1 + R_2 \leq \log_2(1+\frac{P_1+P_2}{N_0}). \tag{9}$$

To achieve this goal, current NOMA leverages SIC to decode the signals from two concurrent users. Without loss of generality, we assume that $P_1 \leq P_2$, the receiver decodes the signal from user 2 first, and then cancels it out from the received signal. After that, the signal from user 1 can be decoded as interference from other user is cancelled. From the capacity perspective, the user 1 can use its full rate as $\log_2(1+\frac{P_1}{N_0})$, and user 2 can have a rate as

$$R_2 = \log_2(1+\frac{P_2}{P_1+N_0}). \tag{10}$$

By doing this, the overall capacity of the two users can be improved compared with OMA schemes.

However, to implement SIC in practice, a strong assumption is needed. In particular, an obvious power gap should exist between the transmitted signals from the two users; otherwise, the SIC cannot separate the signals effectively and obtain the desired capacity gain. Let us use numerical analysis to study this situation. For example, we have two signals at SNR of 5 dB, which means

$$\frac{P_1}{N_0} = \frac{P_2}{N_0} = 5\text{dB}. \tag{11}$$

When the receiver uses SIC to decode the superimposed signal, the SNR for user 2 would be decreased to 0.76, or -1.1 dB, which is undesirable for practical communication systems. Note that this low SNR will appear as long as the received signal powers are similar. To address this problem, I-Talk

releases the constraint of the power gap. We decode the signal in the modulation level so that the signal would be separated in the constellation map instead of in the power domain, and by doing this, the capacity bound of I-Talk approaches $\log_2(1+\frac{P_1+P_2}{N_0})$, as shown in Fig. 14.

Compassion with back-to-back transmissions. First, in the PHY layer, error coding has been an essential part for wireless systems, and many current systems and standards are embracing the blind retransmission to increase the reliability and reduce the cost of unwanted packet losses [48], [49], [50], [51]. To this end, by using two blind back-to-back transmissions without ACK as an example, it would take 4 time slots for two concurrent users, instead of using I-Talk with only 2 time slots, by which we can save a comparable overall transmission time. Since we can decode the superimposed signal and each of the signal copies has been transmitted twice, we can utilize this diversity gain to further improve the decoding performance by our smart combining scheme. Next, ACK feedback and retransmission is a link-layer error recovery solution, which is effective if the residual error rate of the PHY layer is low; otherwise, most packets may require a large number of retransmissions, leading to poor performance and low efficiency. Therefore, in wireless systems, the PHY layer needs to bring down the bit error rate to be sufficiently low using error coding (such as blind retransmission or various error codes). The proposed I-Talk is a PHY-layer solution. It can be combined with link-layer ACK and retransmission to ensure the link-layer performance, which is an important further research issue.

VI. Evaluation

A. Experiment Setting

We build a prototype of I-Talk using USRP N210 embedded with an XCVR2450 daughter board. Each USRP connects to a GPS-Disciplined Oscillator (GPSDO) for the time synchronization. I-Talk is based on the PHY configurations of the IEEE 802.11p standard (i.e. the 5.9 GHz carrier frequency and 10 MHz bandwidth), and is built upon a recent project programmed in GNU-radio [34]. Prototyping in a software-defined radio platform, USRP (one of the most widely used software-defined radio system for research), is to demonstrate the feasibility of the proposed I-Talk solution. With the successful implementation in USRP, we can conclude that the proposed I-Talk is practical and promising.

To evaluate I-Talk in the mobile scenario, experiments with three vehicles are performed on city roads as shown in Fig. 15c. During the experiment, the first and the third vehicles act as the source nodes transmitting signals simultaneously, while the second vehicle is the receiver node (Fig. 15a). The vehicles drove at a maximum speed of 40 km/h and following the normal traffic rules. The setup in one vehicle is shown in Fig. 15b where the communication node is placed on the back seat. We deploy an ECOM9-5500 mag-mount antenna with 9 dBi gain on top of each vehicle, near to the GPS antenna.

B. Overall Performance

Among all superimposed signal decoding approaches, PNC can work well without power control [8], [9], [10] which is desirable for IoT systems. Since PhyCode [11] is the state-of-the-art approach based on PNC and can decode the superimposed signals for NOMA, we evaluate I-Talk in comparison with PhyCode. In particular, PhyCode decodes the superimposed signal in the modulation-level so it requires no power control. However, it assumes that all the constellation points are naturally distinguishable. This assumption can be held only for ideal conditions where no hardware imperfection and complicated channel conditions are taken into consideration. To be fair, we enable two-copy transmissions in PhyCode but without the rotation code, and select the signal copy that can pass the CRC check.

1) Road Test Performance: For the road test in the mobile scenario, we plot the SNR of two concurrent transmitted signals in Fig. 16a, which shows that although the median SNR can be achieved as 18 dB and 11 dB, respectively, the variance of the SNR is very high as some outliers are below 0 dB, resulting in a highly dynamic channel condition. Fig. 16b shows the bit-error-rate (BER) comparison of I-Talk against PhyCode. The BER is calculated in each received packet. Obviously, the performance of I-Talk is $2.73\times$ higher than PhyCode with the median BER of 5.75×10^{-3} over 1.56×10^{-2}. Overall, I-Talk can perform well under mobile scenarios.

2) Packet Level Performance: We evaluate I-Talk from the packet level in terms of the packet reception rate (PRR) and the throughput gain of I-Talk over PhyCode. We use the bit error information from 5000 packets received by the USRP device under different SNR settings. A common channel coding scheme in 802.11p is used, i.e., the CRC-32 algorithm along with convolutional codes at 1/2 code rates. As plotted in Fig. 17a, I-Talk can achieve a higher PRR with a median value of 0.98 than PhyCode with a median value of 0.52, which represents a significant improvement of reliability. Fig. 17d shows that I-Talk achieves a median $1.47\times$ higher throughput gain than PhyCode.

C. Impacts of Practical Factors

To demonstrate that I-Talk can perform well without power control, we evaluated the impact of both the SNR and the SNR ratio of two transmitted signals. To focus on the influence of each parameter, we conducted this experiment in an open space where the GPS signals can be stably received. We collected 500 superimposed packets for each setting. These experiments evaluated our performance in static scenarios.

SNR. As shown in Fig. 17b, we manually tune the SNR of the two transmitters from 5 dB to 15 dB. The BER results of I-Talk and PhyCode are illustrated in Fig. 17e. Clearly, I-Talk outperforms PhyCode under different SNRs. Moreover, as the SNR increases, the performance of I-Talk is much higher than PhyCode. For example, when the SNR is around 15 dB, the BER results of I-Talk and PhyCode are 1.57×10^{-5} and 2.13×10^{-2}, respectively. These results reveal that I-Talk performs well within the typical SNR range (>5 dB [17]).

SNR ratio. To evaluate the SNR ratio influence, we keep the SNR_2 around 12 dB and change the SNR_1 gradually. SNR_1 can be either larger or smaller than SNR_2. In Fig. 17f, we see

This article has been accepted for publication in a future issue of this journal, but has not been fully edited. Content may change prior to final publication. Citation information: DOI 10.1109/TWC.2021.3057864, IEEE Transactions on Wireless Communications

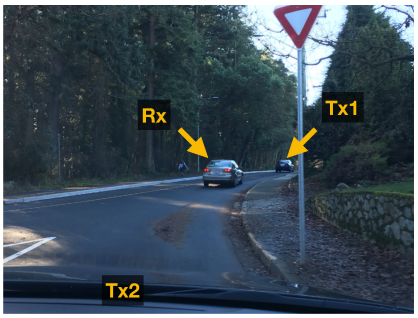

(a) Driving road.

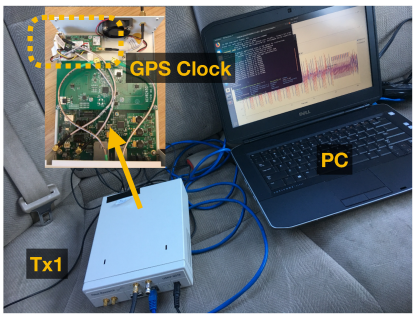

(b) Hardware setup.

(c) Driving map.

Fig. 15: Road test.

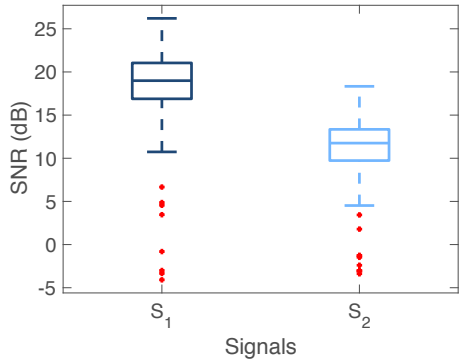

(a) SNR.

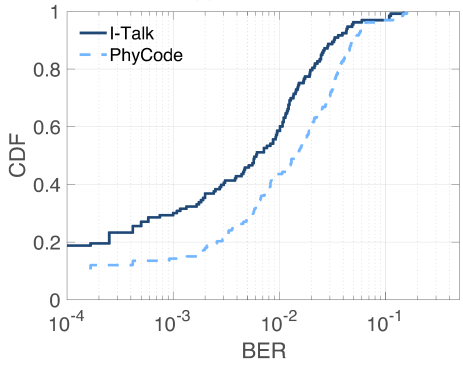

(b) BER.

Fig. 16: Road test results.

that I-Talk still outperforms PhyCode with the varying SNR ratio. The results reveal that I-Talk can perform well over a large range of the SNR ratio without any power control.

D. Evaluation of Smart Combining

We then focus on the other core component of I-Talk, i.e., smart combining. For simplicity, in this experiment, we set SNR_1 as 15 dB and SNR_2 as 12 dB. As shown in Fig. 18, the median BER is 1.6×10^{-2} without applying the smart combining. In contrast, the median BER of I-Talk significantly reduces to 8.33×10^{-5} after applying the smart combining scheme. This result demonstrates that I-Talk can precisely respond to the subcarriers' diversity. Besides, I-Talk outperforms PhyCode even without smart combining. Because I-Talk can still conduct a simple selection scheme with the knowledge of the phase differences compared to PhyCode.

VII. Discussion and Conclusion

A. Discussion

Various modulation schemes. The IoT related communication techniques such as RFID, LoRa, ZigBee and WiFi are attracting the most attention. In particular, RFID, LoRa and ZigBee are operating on narrow-band carriers, designed for applications with low-date-rate, in a range of tens of Kbps to hundreds of Kbps. WiFi signals operates on wide-band carriers with the OFDM technology, achieving a data rate of a few Mbps even with the lowest modulation scheme—BPSK modulation. In this paper, we devote our efforts to enable concurrent transmission of WiFi (IEEE 802.11) signals modulated by BPSK. We believe the data rate provided by the BPSK WiFi signal is sufficient for the majority of IoT applications. Moreover, BPSK modulated signals are more robust to complicated channel conditions, making our scheme feasible for a wider range of applications. On the other hand, a higher order of modulation can provide further enhancement to our scheme in terms of the data rate at the cost of higher complexity. If a future application prefers a higher-order modulation, the idea proposed in this paper can be further extended to support it. This is because the symmetric property among the constellation points still exist, which can ensure a stable decoding performance for I-Talk.

Decoding superimposed for two-user scenarios. Although NOMA was proposed to address a massive number of users, the existing SIC-based NOMA implementations are also focusing on two-user concurrent transmission cases [52], [53], [6], [54], [55]. The underlying reason for this is that maintaining a power gap between users is challenging in mobile environments. For more users, the popular solution is to apply grouping or other scheduling solutions to arrange the two-user NOMA communication only [52], which is beyond the scope of this paper.

A large-scale testbed with many communication nodes. The implementation of our work includes few communication nodes due to the limited number of the experimental devices, i.e., testing vehicles and USRPs. We believe the study of this work can be seen as a solid foundation for further researches, where more devices can be involved.

This article has been accepted for publication in a future issue of this journal, but has not been fully edited. Content may change prior to final publication. Citation information: DOI 10.1109/TWC.2021.3057864, IEEE Transactions on Wireless Communications

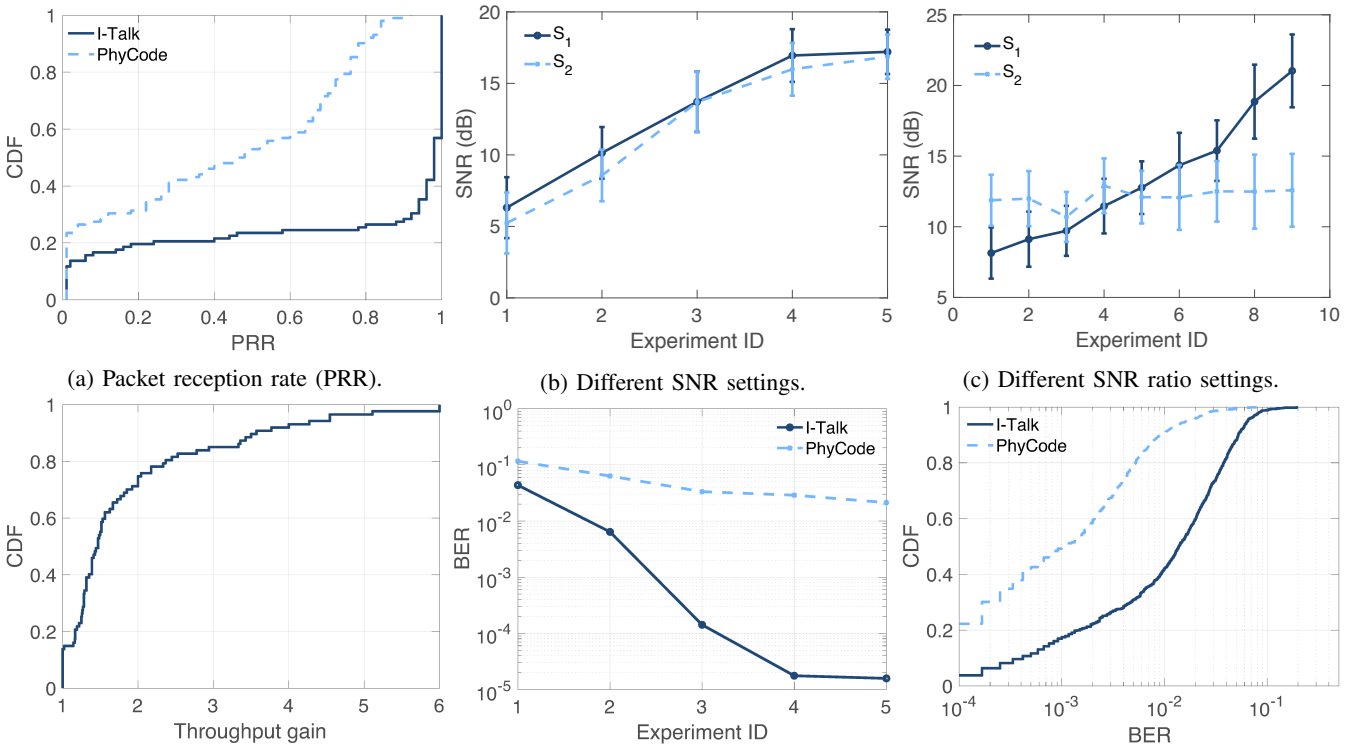

(a) Packet reception rate (PRR).

(b) Different SNR settings.

(c) Different SNR ratio settings.

(d) Throughput gain.

(e) BER under different SNRs.

(f) BER under different SNR ratios.

Fig. 17: Performance evaluation.

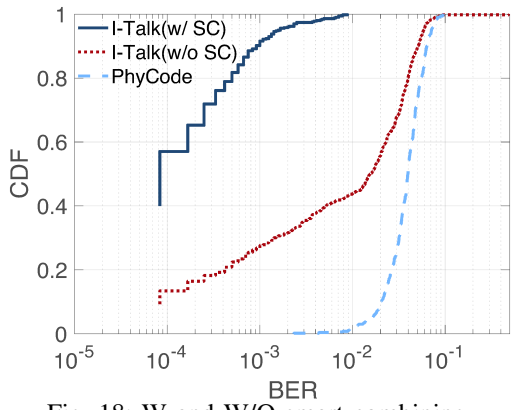

Fig. 18: W and W/O smart combining.

B. Conclusion

In this paper, we propose I-Talk, a new NOMA approach designed for IoT systems that can decode the superimposed signals without power control. I-Talk can achieve high reliability and high throughput in the presence of mobility and hardware imperfections. We design a synthesis channel coefficient together with a diversity transmission and smart combining scheme to track the signal offsets caused by the hardware imperfection and reduce the decoding error under the mobile channel conditions. We demonstrate the performance of I-Talk with a software-defined radio platform in the mobile scenario. The results reveal that I-Talk outperforms the state-of-the-art scheme in terms of a higher reliability and a higher throughput gain.

References

[1] I. Yaqoob, I. A. T. Hashem, A. Ahmed, S. A. Kazmi, and C. S. Hong, "Internet of things forensics: Recent advances, taxonomy, requirements, and open challenges," *Elsevier Future Generation Computer Systems*, vol. 92, pp. 265–275, 2019.

[2] "Cisco annual Internet report (2018–2023) white paper," *Cisco white paper*, 2020.

[3] A. A. Khan, M. H. Rehmani, and A. Rachedi, "Cognitive-radio-based Internet of things: Applications, architectures, spectrum related functionalities, and future research directions," *IEEE Wireless Communications*, vol. 24, no. 3, pp. 17–25, 2017.

[4] X. Liu, M. Jia, X. Zhang, and W. Lu, "A novel multichannel Internet of things based on dynamic spectrum sharing in 5G communication," *IEEE Internet of Things Journal*, vol. 6, no. 4, pp. 5962–5970, 2018.

[5] D. Tse and P. Viswanath, *Fundamentals of wireless communication*. Cambridge university press, 2005.

[6] Y. Saito, Y. Kishiyama, A. Benjebbour, T. Nakamura, A. Li, and K. Higuchi, "Non-Orthogonal Multiple Access (NOMA) for cellular future radio access," in *2013 IEEE 77th Vehicular Technology Conference (VTC Spring)*. IEEE, 2013, pp. 1–5.

[7] L. Dai, B. Wang, Y. Yuan, S. Han, I. Chih-Lin, and Z. Wang, "Non-orthogonal multiple access for 5G: Solutions, challenges, opportunities, and future research trends," *IEEE Communications Magazine*, vol. 53, no. 9, pp. 74–81, 2015.

[8] S. Zhang, S. C. Liew, and P. P. Lam, "Hot topic: Physical-layer network coding," in *Proceedings of the 12th annual international conference on Mobile computing and networking*. ACM, 2006, pp. 358–365.

[9] L. Lu, T. Wang, S. C. Liew, and S. Zhang, "Implementation of physical-layer network coding," *Elsevier Physical Communication*, vol. 6, pp. 74–87, 2013.

[10] L. You, S. C. Liew, and L. Lu, "Reliable physical-layer network coding supporting real applications," *IEEE Transactions on Mobile Computing*, vol. 16, no. 8, pp. 2334–2350, 2016.

[11] W. Cui, C. Liu, L. Cai, and J. Pan, "Phycode: A practical wireless communication system exploiting superimposed signals," in *ICC 2019-2019 IEEE International Conference on Communications (ICC)*. IEEE, 2019, pp. 1–6.

[12] T. Das, L. Chen, R. Kundu, A. Bakshi, P. Sinha, K. Srinivasan, G. Bansal, and T. Shimizu, "Corecast: Collision resilient broadcasting

in vehicular networks," in *Proceedings of the 16th Annual International Conference on Mobile Systems, Applications, and Services*. ACM, 2018, pp. 217–229.

[13] W. Zhou, T. Das, L. Chen, K. Srinivasan, and P. Sinha, "Basic: Backbone-assisted successive interference cancellation," in *Proceedings of the 22nd Annual International Conference on Mobile Computing and Networking*. ACM, 2016, pp. 149–161.

[14] H. Zhang, L. Zheng, and L. Cai, "Design and analysis of hierarchical physical layer network coding," *IEEE Transactions on Wireless Communications*, vol. 16, no. 12, pp. 7966–7981, 2017.

[15] H. Zhang and L. Cai, "Design of channel coded heterogeneous modulation physical layer network coding," *IEEE Transactions on Vehicular Technology*, vol. 67, no. 3, pp. 2219–2230, 2017.

[16] ——, "Bi-directional multi-hop wireless pipeline using physical-layer network coding," *IEEE Transactions on Wireless Communications*, vol. 16, no. 12, pp. 7950–7965, 2017.

[17] S. Katti, S. Gollakota, and D. Katabi, "Embracing wireless interference: Analog network coding," in *ACM SIGCOMM Computer Communication Review*, vol. 37, no. 4. ACM, 2007, pp. 397–408.

[18] M. Jin, Y. He, X. Meng, D. Fang, and X. Chen, "Parallel backscatter in the wild: When burstiness and randomness play with you," in *Proceedings of the 24th Annual International Conference on Mobile Computing and Networking*. ACM, 2018, pp. 471–485.

[19] B. Ghena, J. Adkins, L. Shangguan, K. Jamieson, P. Levis, and P. Dutta, "Challenge: Unlicensed lpwans are not yet the path to ubiquitous connectivity," in *The 25th Annual International Conference on Mobile Computing and Networking*. ACM, 2019, p. 43.

[20] L. Kong and X. Liu, "mzig: Enabling multi-packet reception in ZigBee," in *Proceedings of the 21st annual international conference on mobile computing and networking*. ACM, 2015, pp. 552–565.

[21] S. M. Alamouti, "A simple transmit diversity technique for wireless communications," *IEEE Journal on selected areas in communications*, vol. 16, no. 8, pp. 1451–1458, 1998.

[22] V. Tarokh, H. Jafarkhani, and A. R. Calderbank, "Space-time block codes from orthogonal designs," *IEEE Transactions on Information theory*, vol. 45, no. 5, pp. 1456–1467, 1999.

[23] H. Jafarkhani, "A quasi-orthogonal space-time block code," *IEEE Transactions on Communications*, vol. 49, no. 1, pp. 1–4, 2001.

[24] J. Bae, K.-H. Lee, J. M. Kim, B. C. Jung, and J. Joung, "Performance analysis of uplink NOMA-IoT networks with space-time line code," in *2019 IEEE 90th Vehicular Technology Conference (VTC2019-Fall)*. IEEE, 2019, pp. 1–5.

[25] H. Rahul, H. Hassanieh, and D. Katabi, "SourceSync: A distributed wireless architecture for exploiting sender diversity," *ACM SIGCOMM Computer Communication Review*, vol. 41, no. 4, pp. 171–182, 2011.

[26] H. S. Rahul, S. Kumar, and D. Katabi, "JMB: Scaling wireless capacity with user demands," *ACM SIGCOMM Computer Communication Review*, vol. 42, no. 4, pp. 235–246, 2012.

[27] E. Hamed, H. Rahul, M. A. Abdelghany, and D. Katabi, "Real-time distributed MIMO systems," in *Proceedings of the 2016 ACM SIGCOMM Conference*, 2016, pp. 412–425.

[28] S. Biswas and R. Morris, "Opportunistic routing in multi-hop wireless networks," *ACM SIGCOMM Computer Communication Review*, vol. 34, no. 1, pp. 69–74, 2004.

[29] I. F. Akyildiz and M. C. Vuran, *Wireless Sensor Networks*. John Wiley & Sons, 2010, vol. 4.

[30] J. Schmitz, F. Bartsch, M. Hernández, and R. Mathar, "Distributed software defined radio testbed for real-time emitter localization and tracking," in *2017 IEEE International Conference on Communications Workshops (ICC Workshops)*. IEEE, 2017, pp. 1246–1252.

[31] R. Zhao, F. Zhu, Y. Feng, S. Peng, X. Tian, H. Yu, and X. Wang, "OFDMA-Enabled Wi-Fi backscatter," in *The 25th Annual International Conference on Mobile Computing and Networking*. ACM, 2019, pp. 1–15.

[32] M. Kotaru, K. Joshi, D. Bharadia, and S. Katti, "Spotfi: Decimeter level localization using WiFi," in *ACM SIGCOMM computer communication review*, vol. 45, no. 4. ACM, 2015, pp. 269–282.

[33] H. Meyr, M. Moeneclaey, and S. Fechtel, *Digital communication receivers: Synchronization, channel estimation, and signal processing*. John Wiley & Sons, Inc., 1997.

[34] B. Bloessl, M. Segata, C. Sommer, and F. Dressler, "Performance assessment of IEEE 802.11 p with an open source SDR-based prototype," *IEEE transactions on mobile computing*, vol. 17, no. 5, pp. 1162–1175, 2017.

[35] H. Pan, L. Lu, and S. C. Liew, "Practical power-balanced non-orthogonal multiple access," *IEEE Journal on Selected Areas in Communications*, vol. 35, no. 10, pp. 2312–2327, 2017.

[36] ——, "Network-coded multiple access with high-order modulations," *IEEE Transactions on Vehicular Technology*, vol. 66, no. 11, pp. 9776–9792, 2017.

[37] H. Pan, S. C. Liew, J. Liang, Y. Shao, and L. Lu, "Network-coded multiple access on unmanned aerial vehicle," *IEEE Journal on Selected Areas in Communications*, vol. 36, no. 9, pp. 2071–2086, 2018.

[38] A. Y.-C. Peng, S. Yousefi, and I.-M. Kim, "On error analysis and distributed phase steering for wireless network coding over fading channels," *IEEE Transactions on Wireless Communications*, vol. 8, no. 11, pp. 5639–5649, 2009.

[39] M. Park, I. Choi, and I. Lee, "Exact BER analysis of physical layer network coding for two-way relay channels," in *2011 IEEE 73rd Vehicular Technology Conference (VTC Spring)*. IEEE, 2011, pp. 1–5.

[40] T. H. Lee and A. Hajimiri, "Oscillator phase noise: A tutorial," *IEEE Journal of Solid-State Circuits*, vol. 35, no. 3, pp. 326–336, 2000.

[41] V. Syrjala, M. Valkama, N. N. Tchamov, and J. Rinne, "Phase noise modelling and mitigation techniques in OFDM communications systems," in *2009 Wireless Telecommunications Symposium*. IEEE, 2009, pp. 1–7.

[42] T. K. Lo, "Maximum ratio transmission," in *1999 IEEE International Conference on Communications (Cat. No. 99CH36311)*, vol. 2. IEEE, 1999, pp. 1310–1314.

[43] A. Goldsmith, *Wireless communications*. Cambridge university press, 2005.

[44] H. A. Mahmoud and H. Arslan, "Error vector magnitude to snr conversion for nondata-aided receivers," *IEEE Transactions on Wireless Communications*, vol. 8, no. 5, pp. 2694–2704, 2009.

[45] A. Georgiadis, "Gain, phase imbalance, and phase noise effects on error vector magnitude," *IEEE Transactions on Vehicular Technology*, vol. 53, no. 2, pp. 443–449, 2004.

[46] D. Halperin, W. Hu, A. Sheth, and D. Wetherall, "Predictable 802.11 packet delivery from wireless channel measurements," *ACM SIGCOMM Computer Communication Review*, vol. 41, no. 4, pp. 159–170, 2011.

[47] J. Wang, H. Jiang, J. Xiong, K. Jamieson, X. Chen, D. Fang, and B. Xie, "LiFS: Low human-effort, device-free localization with fine-grained subcarrier information," in *Proceedings of the 22nd Annual International Conference on Mobile Computing and Networking*. ACM, 2016, pp. 243–256.

[48] Y. Li and L. Cai, "Cooperative device-to-device communication for uplink transmission in cellular system," *IEEE Transactions on Wireless Communications*, vol. 17, no. 6, pp. 3903–3917, 2018.

[49] G. T. 36.888, "Study on provision of low-cost Machine-Type Communications (MTC) user equipments (UEs) based on LTE." 2013.

[50] S.-M. Oh and J. Shin, "An efficient small data transmission scheme in the 3GPP NB-IoT system," *IEEE Communications Letters*, vol. 21, no. 3, pp. 660–663, 2016.

[51] M. Shirvanimoghaddam, M. Dohler, and S. J. Johnson, "Massive non-orthogonal multiple access for cellular IoT: Potentials and limitations," *IEEE Communications Magazine*, vol. 55, no. 9, pp. 55–61, 2017.

[52] S. R. Islam, M. Zeng, O. A. Dobre, and K.-S. Kwak, "Nonorthogonal Multiple Access (NOMA): How it meets 5G and beyond," *Wiley 5G Ref: The Essential 5G Reference Online*, pp. 1–28, 2019.

[53] Y. Liu, Z. Qin, M. Elkashlan, Z. Ding, A. Nallanathan, and L. Hanzo, "Non-orthogonal multiple access for 5G and beyond," *Proceedings of the IEEE*, vol. 105, no. 12, pp. 2347–2381, 2017.

[54] X. Xiong, W. Xiang, K. Zheng, H. Shen, and X. Wei, "An open source sdr-based noma system for 5G networks," *IEEE Wireless Communications*, vol. 22, no. 6, pp. 24–32, 2015.

[55] A. Benjebbour, K. Saito, A. Li, Y. Kishiyama, and T. Nakamura, "Non-orthogonal multiple access (NOMA): Concept, performance evaluation and experimental trials," in *2015 International Conference on Wireless Networks and Mobile Communications (WINCOM)*. IEEE, 2015, pp. 1–6.

Wen Cui (Student Member, IEEE) received the B.S. degree in computer science from Xi'an University of Science and Technology, Xi'an, China, and the M.S. degree in software engineering from Northwest University, Xi'an, China, in 2013 and 2016, respectively. He is working toward the Ph.D. degree in the Department of Electrical and Computer Engineering, University of Victoria, Victoria, Canada. His research interests include wireless communications, Internet-of-things.

Chen Liu received the B.S., M.S. and Ph.D. degrees in computer science from Northwest University, Xi'an, China, in 2009, 2012 and 2016, respectively. She is currently an engineer with Northwest University and a postdoctoral research fellow with the Department of Electrical and Computer Engineering at the University of Victoria. Her research interests include wireless sensing, localization and wireless networks.

Wenjun Yang (Student Member, IEEE) received his M.S. degree in Information Science and Engineering from the Hunan Normal University, Changsha, China, in 2019. He is currently a Ph.D. student in the Department of Electrical & Computer Engineering at the University of Victoria, Victoria, Canada. His current research is on the next generation of network architecture and related issues such as multipath TCP, mulithoming, mobility, and satellite network.

Lin Cai (Fellow, IEEE) Lin Cai (S'00-M'06-SM'10-F'20) received her M.A.Sc. and Ph.D. degrees (awarded Outstanding Achievement in Graduate Studies) in electrical and computer engineering from the University of Waterloo, Waterloo, Canada, in 2002 and 2005, respectively. Since 2005, she has been with the Department of Electrical & Computer Engineering at the University of Victoria, and she is currently a Professor. She is an NSERC E.W.R. Steacie Memorial Fellow and an IEEE Fellow. In 2020, she was elected as a Member of the Royal Society of Canada's College of New Scholars, Artists and Scientists. She was also elected as a 2020 "Star in Computer Networking and Communications" by N2Women. Her research interests span several areas in communications and networking, with a focus on network protocol and architecture design supporting emerging multimedia traffic and the Internet of Things. She was a recipient of the NSERC Discovery Accelerator Supplement (DAS) Grants in 2010 and 2015, respectively, and the Best Paper Awards of IEEE ICC 2008 and IEEE WCNC 2011. She has co-founded and chaired the IEEE Victoria Section Vehicular Technology and Communications Joint Societies Chapter. She has been elected to serve the IEEE Vehicular Technology Society Board of Governors, 2019 - 2021. She has served as an area editor for IEEE Transactions on Vehicular Technology, a member of the Steering Committee of the IEEE Transactions on Big Data (TBD) and IEEE Transactions on Cloud Computing (TCC), an Associate Editor of the IEEE Internet of Things Journal, IEEE Transactions on Wireless Communications, IEEE Transactions on Vehicular Technology, IEEE Transactions on Communications, EURASIP Journal on Wireless Communications and Networking, International Journal of Sensor Networks, and Journal of Communications and Networks (JCN), and as the Distinguished Lecturer of the IEEE VTS Society. She has served as a TPC co-chair for IEEE VTC2020-Fall, and a TPC symposium co-chair for IEEE Globecom'10 and Globecom'13. She is a registered professional engineer in British Columbia, Canada.